Schizophrenia Bulletin vol. 49 no. 5 pp. 1325–1335, 2023
https://doi.org/10.1093/schbul/sbad057
Advance Access publication April 20, 2023

Evidence of Neurovascular Water Exchange and Endothelial Vascular Dysfunction in Schizophrenia: An Exploratory Study

Eric L. Goldwaser[1,8,*], Danny J. J. Wang[2,3], Bhim M. Adhikari[1], Joshua Chiappelli[1], Xingfeng Shao[2], Jiaao Yu[4], Tong Lu[4], Shuo Chen[1,4], Wyatt Marshall[1], Alexa Yuen[1], Mark Kvarta[1], Yizhou Ma[1], Xiaoming Du[1], Si Gao[1], Osamah Saeedi[5], Heather Bruce[1], Patrick Donnelly[1], Hugh O'Neill[1], Alan R. Shuldiner[6], Braxton D. Mitchell[6,7], Peter Kochunov[1], and L. Elliot Hong[1,*]

[1]Maryland Psychiatric Research Center, Department of Psychiatry, University of Maryland School of Medicine, Baltimore, MD, USA; [2]Laboratory of FMRI Technology (LOFT), Mark & Mary Stevens Nueroimaging and Informatics Institute, Keck School of Medicine, University of Southern California, Los Angeles, CA, USA; [3]Department of Neurology, Keck School of Medicine, University of Southern California, Los Angeles, CA, USA; [4]Department of Mathematics, University of Maryland, College Park, MD, USA; [5]Department of Ophthalmology and Visual Sciences, University of Maryland Medical Center, Baltimore, MD, USA; [6]Department of Medicine, University of Maryland School of Medicine, Baltimore, MD, USA; [7]Geriatrics Research and Education Clinical Center, Baltimore Veterans Administration Medical Center, Baltimore, MD, USA; [8]Present address: Department of Psychiatry, Weill Cornell Medicine, 1165 York Avenue, New York, NY, USA

*To whom correspondence should be addressed; Maryland Psychiatric Research Center, P.O. Box 21247, Baltimore, MD 21228, USA; tel: 201-406-3670, e-mail: bxt9001@med.cornell.edu; ehong@som.umaryland.edu

***Background and Hypothesis*: Mounting evidence supports cerebrovascular contributions to schizophrenia spectrum disorder (SSD) but with unknown mechanisms. The blood–brain barrier (BBB) is at the nexus of neural-vascular exchanges, tasked with regulating cerebral homeostasis. BBB abnormalities in SSD, if any, are likely more subtle compared to typical neurological insults and imaging measures that assess large molecule BBB leakage in major neurological events may not be sensitive enough to directly examine BBB abnormalities in SSD. *Study Design*: We tested the hypothesis that neurovascular water exchange (Kw) measured by non-invasive diffusion-prepared arterial spin label MRI (n = 27 healthy controls [HC], n = 32 SSD) is impaired in SSD and associated with clinical symptoms. Peripheral vascular endothelial health was examined by brachial artery flow-mediated dilation (n = 44 HC, n = 37 SSD) to examine whether centrally measured Kw is related to endothelial functions. *Study Results*. Whole-brain average Kw was significantly reduced in SSD (P = .007). Exploratory analyses demonstrated neurovascular water exchange reductions in the right parietal lobe, including the supramarginal gyrus (P = .002) and postcentral gyrus (P = .008). Reduced right superior corona radiata (P = .001) and right angular gyrus Kw (P = .006) was associated with negative symptoms. Peripheral endothelial function was also significantly reduced in SSD (P = .0001). Kw in 94% of brain regions in HC positively associated with peripheral endothelial function, which was not observed in SSD, where the correlation was inversed in 52% of brain regions. *Conclusions*: This study provides initial evidence of neurovascular water exchange abnormalities, which appeared clinically associated, especially with negative symptoms, in schizophrenia.**

Key words: blood–brain barrier/diffusion-prepared arterial spin label/psychosis/vasculature/flow-mediated dilation/neurovascular unit

Introduction

Schizophrenia spectrum disorder (SSD) is a severe form of psychopathology, yet cerebral mechanisms are poorly understood. A crucial structure regulating cerebral integrity is the blood–brain barrier (BBB), composed of endothelial cells and surrounding astrocytes and pericytes, tasked to maintain cerebral homeostasis through the functional neurovascular unit. Postmortem studies support BBB deficits in SSD,[1,2] particularly endothelial and astrocytic subcomponents.[3] However, limited knowledge exists about clinical relevance of putative BBB abnormalities due to difficulties directly assessing BBB dysfunction clinically in SSD patients.

BBB compromise is typically assessed using dynamic contrast-enhanced MRI (DCE-MRI), measuring large-molecule contrast leakage in neurological insults. No significant abnormalities were identified in first-episode or chronic SSD patients using this technique.[4] Other methods include C^{11}-verapamil positron emission tomography

(PET) and cerebrospinal fluid (CSF)/plasma ratios of fluid biomarkers but are limited by their invasiveness. The recently developed diffusion-prepared arterial spin labeling (DP-ASL) technique takes advantage of the much smaller water molecule for detecting water exchange (Kw) between brain capillary and neuronal compartments.[5,6] Illnesses with known BBB disruptions, like obstructive sleep apnea[6] and elderly at-risk for Alzheimer's disease, showed reduced Kw,[6–8] thought to reflect hypofunctional or impaired active water transport. In rodent models of cerebrovascular injury, this technique more sensitively detected BBB damage than contrast-based imaging,[9,10] suggesting a new, clinically accessible approach to understand brain capillary-parenchyma exchange abnormalities. Based on studies comparing DP-ASL and DCE-MRI,[11] the mechanism underlying Kw and standard BBB permeability measure (K_{trans}) is likely different.[7,8,12,13] Reduced Kw may mainly reflect impaired transport of water across the neurovascular unit, which is related to aquaporin-4 (AQP-4) function rather than abnormal passive permeability of water or large molecules across endothelium.

Core clinical features of SSD, including positive/negative symptoms and cognitive deficits, have been associated with cerebrovascular abnormalities in traditional cerebral blood flow studies.[14,15] Positive symptoms tend to associate with hypo-/hyper-perfusion in different brain regions, but negative symptoms almost exclusively associate with hypoperfusion, particularly in frontoparietal areas.[14,16] Negative symptoms are also associated with reduced frontoparietal activation during decision and attention tasks[17,18] and with abnormalities in local temporo-parietal networks.[19,20] The underlying mechanisms remain obscure, but consistent links between negative symptoms and hypoperfusion[14,15,21] alludes to a neurovascular dysfunction not yet explored.

We aimed to test the hypothesis that brain vascular-neural water exchange functions measured by Kw would be impaired in SSD, influencing neuronal function in regions associated with negative symptoms. Furthermore, as the major vascular structure to regulate capillary–neural tissue exchange is the endothelial lining, it would be useful to specifically examine BBB endothelial functions. While no such method exists clinically, brachial artery flow-mediated dilation (FMD) is a standard measure to assess peripheral nitric oxide-mediated endothelial function, which strongly predicts cardiovascular disease.[22–24] Nitric oxide biosynthesis and related molecular nitric oxide pathways have been found aberrant in SSD,[25,26] although it is previously unclear whether a clinical measure like FMD may index these dysfunctional pathways. FMD occurs following brachial artery occlusive stress, inducing endothelial dilation secondary to shear stress from hyperemic responses.[27–29] The degree of endothelial dilation reflects vascular health, whereby reduced dilation represents endothelial impairment, as in many disease states,[30,31] and may manifest similarly across body and brain. It is unknown whether peripheral FMD can predict neurovascular function.

Although the endothelial lining is universally present in central and peripheral vessels, regional characteristics exist with notable differences.[32] Commonalities in dysfunction may register across vascular systems nonetheless and understanding ways in which they may relate can serve the development of important proxy measures to index neurovascular integrity. Therefore, we aimed to also test a second hypothesis that endothelial dysfunctions (measured by FMD) are associated with cerebral capillary-tissue water exchange abnormalities (measured by Kw). To summarize, we hypothesized that brain capillary-tissue exchange functions would be impaired in SSD and be clinically relevant. We proposed to investigate this hypothesis using two noninvasive approaches: central capillary-neural tissue water exchange (Kw) and peripheral endothelial function (FMD).

Methods

Participants

Forty-four participants with SSD and 37 healthy controls (HC) were recruited from mental health clinics in Baltimore, MD and media advertisements; all completed vascular testing and 32 SSD and 27 HC completed brain imaging. The Structured Clinical Interview for *DSM-5* was utilized to obtain diagnoses of either schizophrenia or schizoaffective disorder (SSD). HC had no current major mental illness; however, past single episode of depression/anxiety was allowed. Current or past major medical illnesses, head injury with cognitive sequelae, intellectual disability, or current substance abuse were exclusionary. Negative symptoms were assessed using the Brief Negative Symptom Scale (BNSS).[33] Positive and negative symptoms were further assessed using the respective subscales in the Brief Psychiatric Rating Scale (BPRS).[34] Both scales are clinician-administered, based on semi-structured interviews, and all raters were formally trained with multiple videotaped case interviews until raters achieved acceptable reliability. Cognitive performance in working memory[35] and processing speed[36] was assessed using spatial span and digit-symbol coding tasks, respectively. Antipsychotic doses were converted into chlorpromazine (CPZ) equivalents (table 1). Participants signed informed consent approved by the University of Maryland Baltimore IRB.

Diffusion-Prepared Pseudo-Continuous Arterial Spin Label (DP-ASL) Imaging

Imaging was obtained using a Siemens 3T PRISMA scanner with a 64-channel head-coil. Imaging parameters were the following: field-of-view = 224 mm; matrix size = 64 × 64; 12 axial slices (10% oversampling); resolution = 3.5 × 3.5 × 8 mm; 3D gradient and spin

Table 1. Participant Clinical and Demographic Information

	Control (n = 37)	SSD (n = 44)	t or χ^2 values	P-value
Age [years] (*SD*)	39.5 (15.8)	37.4 (13.2)	0.5	.6
Sex (M:F)	15:22	34:9	12.4	1×10^{-3}
BMI (*SD*)	27.1 (6.2)	30.6 (6.0)	−2.3	.02
Current smoker (%)	21.2	33.3	1.3	.25
CPZ equivalents [a]	n/a	616.6 (100)	n/a	n/a
BPRS, psychosis (*SD*)	n/a	7.36 (3.34)	n/a	n/a
BPRS, negative subscale (*SD*)	n/a	8.14 (3.55)	n/a	n/a
BNSS, total (*SD*)	n/a	27.17 (15.5)	n/a	n/a
Room temperature [b] (°F) (*SD*)	75.0 (2.3)	74.0 (3.6)	1.3	.2
Room humidity [b] (%) (*SD*)	29.3 (11.6)	34.7 (13.4)	−1.8	.08

[a]Antipsychotic medication dose is provided in chlorpromazine equivalents (CPZ) (milligrams/day).
[b]Recorded during flow-mediated dilation testing.

echo (GRASE) readout; bandwidth = 3,25 Hz/pixel; TE = 36.5 ms; TR = 4,000 ms; label duration = 1,500 ms; centric ordering; and timing of background suppression was optimized .[5] A 2-stage approach for Kw measurement was employed with a total scan time of 10 minutes,[37] namely a flow encoding arterial spin tagging scan at post-labeling delay (PLD) = 900 ms with b = 0 and 10 s/mm^2 for estimating arterial transit time (ATT),[38] and a second scan at PLD = 1,800 ms with b = 0 and 50 s/mm^2 for estimating Kw. Cerebral blood flow (mL/100 g/min) was quantified from signals acquired at PLD = 1,800 ms without diffusion preparation.

Images were corrected for head motion off-line using SPM12 (Wellcome Trust Centre for Neuroimaging, UCL). Kw maps were calculated using LOFT BBB Toolbox including motion correction, skull stripping, and quality assurance procedures. Two subjects with unusable data due to registration failures were excluded. A total-generalized-variation[39] regularized single-pass-approximation model[37] was applied for Kw calculation using the tissue/capillary fraction of ASL signal at PLD = 1,800 ms, incorporating ATT, arterial blood T1 (1,660 ms[40]), and brain tissue T1 as inputs.[5] Voxel-wise T1 map was fitted from background suppressed control images. Data were processed using FSL Bayesian Inference for ASL (BASIL) pipeline which fits the multipoint PLD kinetic curve model to measure absolute CBF (mL/100 g/min) after partial volume correction derived from high-resolution T1w data. Equilibrium magnetization (M0) images were collected using a TR = 10 s, sufficiently long for T1 relaxation of blood-bound water (T1 = 2 s). Theoretically, the kw metric represents a ratio of capillary permeability surface area product of water (PSw) by capillary volume (Vc).[37] It is the reciprocal of BBB water exchange time (1/water exchange time); therefore, the faster water exchanges across the BBB into brain tissue, the higher Kw and vice versa. This estimates the water exchange rate across the BBB, and is reported in studies tabulated in supplementary table 1.[5–11,37] Previous test–retest DP-ASL scans have shown excellent reproducibility 6 weeks apart for Kw measurements,[11] with intraclass correlation coefficient (ICC) = 0.75.

The primary measure was the whole-brain average Kw between SSD and HC. If significant group differences were found, exploratory analyses were then performed to understand relationships between Kw and underlying brain regions, clinical symptoms, and demographic characteristics. Unlike previous studies, a more detailed brain template, EvePM,[41] was used to explore regional effects in 107 regions. Regions missing Kw data in > 20% of voxels in > 50% of participants were excluded, comprising the bilateral pons, pontine crossing tract, medulla, and cerebellum, leaving 99 regions. As most regions still have missing values in variable numbers of voxels,[42] multivariate multiple imputation by chained equations (MICE)[43] was used for imputation. The full conditional specification in MICE was modified with an updated covariance based on the Gaussian process due to the high-dimensionality property of the brain imaging voxels.[44] The modified MICE method attained imputed values with reduced bias and dispersion and much improved computational efficiency.

Flow-Mediated Dilation (FMD) Testing

Practice guidelines for FMD which were followed,[22,27–29] including standard timing of dilation measurement.[45,46] Participants were asked to fast for 8 hours before testing, refrain from exercise, caffeine, and smoking/nicotine. All testing occurred between 07:00 and 11:00 am. Morning medications and vitamins/supplements were held until after testing. Participants rested for 15 minutes, with lights dimmed, and room temperature and humidity controlled prior to testing.

FMD was measured using standard ultrasound equipment (Philips iE33) and manufacturer software.[27,28,47] Brachial artery was imaged above the antecubital fossa in the longitudinal plane, with clear anterior and posterior intimal surfaces for continuous 2D-grayscale imaging. A 90° isonation angle, horizontally displayed, fully patent lumen,

without scanhead malrotations or 2D beam-steering was visualized. A segment of 1.5 × 1 cm zoom-box was placed over a segment of the artery with fiduciary anatomic markers for imaging. 3-lead ECG (lead II configuration) was positioned to align R-waves along cardiac cycles for consistency. Occlusion was created by a sphygmomanometer cuff on the proximal arm inflated to 50 mmHg suprasystolic pressure for 5 minutes. Images were obtained at baseline, and 1, 3, and 5 minutes post-cuff deflation. FMD was calculated by subtracting vessel size prior to and 1 minute after the occlusion period as percentage change.[27] Normality was achieved by performing Box-Cox transformation. Images were manually measured by a blinded, trained rater (PD).[48] For each rater, 100 supervised experiments were performed prior to data collection. Interrater reliability was established by using images from baseline and 1-minute post-occlusive diameter in 14 participants (28 images total) to reach ICC ≥ 0.90 between a rater and the "gold standard" measured by the sonographer. Averaged ICC was 0.93. For maintaining continuous data acquisition and scoring competency, ~10% of all images were periodically reviewed for quality assurance.

Statistical Analysis

Group differences were examined with analysis of variance (ANOVA) or χ^2. Primary measures of whole-brain average Kw and FMD were compared with age and sex covaried in all analyses. If the primary whole-brain comparison was significant after FDR correction, regional effects were explored. The effect size for whole-brain average Kw was used to calculate the power needed to compare for 99 regions, which suggested that the current sample was not adequately sized to meet the significance thresholds for regional analysis of 99 regions, and as such, an arbitrary alpha value of 0.01 was used for these exploratory, hypothesis-generating analyses. Similarly, relationships between whole-brain average Kw and FMD were examined using partial correlations as the primary analysis, with regional correlational analyses as exploratory. Potential confounding effects from age, sex, smoking, cardiovascular measures (systolic and diastolic blood pressure, resting heart rate), and body mass index were evaluated in Kw and FMD separately. Partial correlation coefficient group differences were compared using Fisher's *r*-to-*z* transformation. All tests were 2-tailed.

Results

Brain Water Exchange Measures

Groups were not significantly different in age but different in sex ratio (**table 1**). Whole-brain averaged Kw was significantly reduced in SSD compared with HC ($P = .007$; **figure 1A**). No significant group differences were observed in left or right hemisphere average Kw ($P = .08$, $P = .07$, respectively) and we used only whole-brain average Kw in subsequent analysis. In comparison, whole-brain averaged cerebral blood flow (CBF) and average arterial transit time (ATT) did not differ significantly between groups ($P = .9$). Kw was therefore the focus of subsequent region-level analyses. Significant reductions (uncorrected) in Kw were found in the right supramarginal gyrus ($P = .002$) and the right postcentral gyrus ($P = .008$) in SSD compared to HC, both at the right parietal lobe (figure 1B, supplementary figure 1).

Relationship between Kw and Clinical Symptoms

Negative symptoms measured by BNSS score were inversely correlated with Kw in ~59% of brain regions

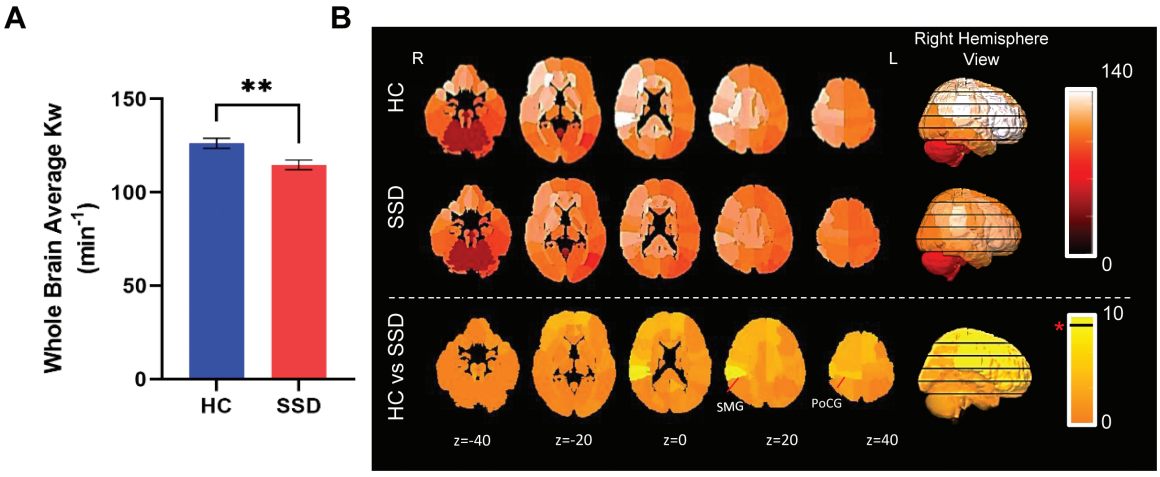

Fig. 1. Whole brain and regional water exchange measures gathered from the diffusion-prepared arterial spin labeling. (A) Whole brain average group differences on water exchange (Kw) (SD). (B) Raw values of Kw were plotted in 99 regions for HC (top panel) and SSD (middle panel), and *t*-value map of the group comparisons using univariate analysis of variance covarying age and sex (bottom panel). Values in the images are the z-coordinates. Horizontal black line in the color legend indicates color corresponds to significant *t*-value. * $P < .01$. R: right; L: left. Error bars are SEM.

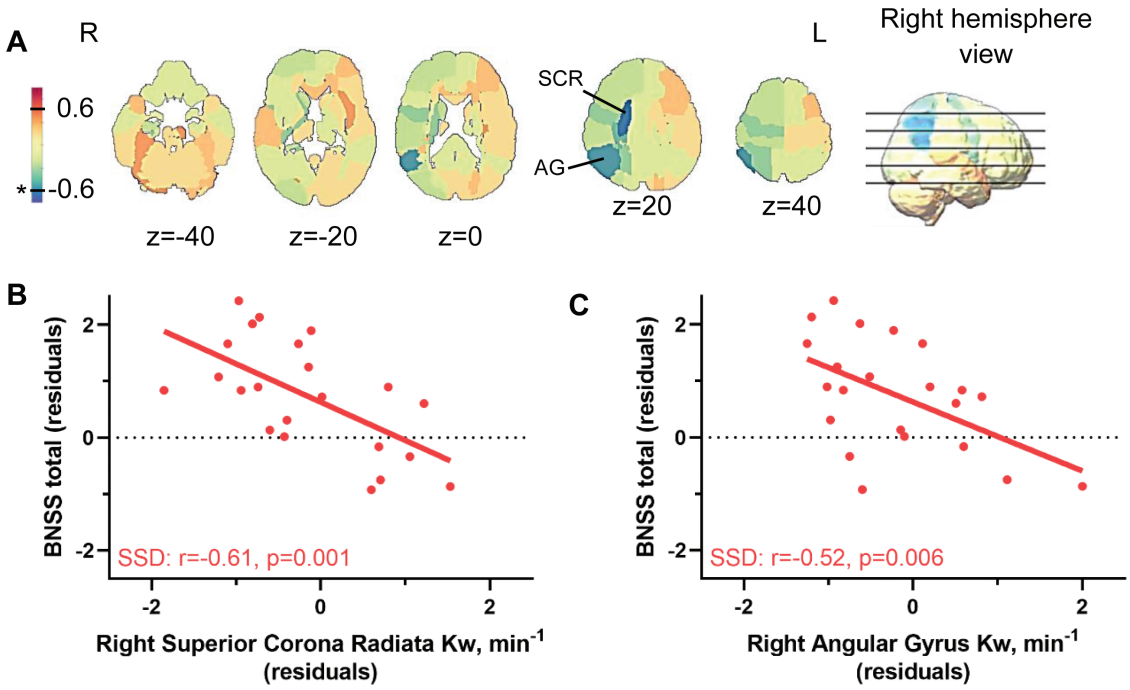

Fig. 2. Negative symptoms associated with regional Kw measurements. (A) Brief negative symptom scale (BNSS) and Kw partial Pearson's correlation r-map in SSD, age and sex covaried. Color bar corresponds to negative (colder colors) and positive (warmer colors) correlations across regions. Two regions, the superior corona radiata (SCR) and the angular gyrus (AG), both on the right, were used to generate (B) and (C), respectively. * $P < .01$.

(**figure 2A**), with two regions significant: right superior corona radiata ($r = -0.61$, $P = .001$) and angular gyrus ($r = -0.52$, $P = .006$; **figures 2B and 2C**, respectively). The superior corona radiata connects parietal lobe to other brain regions, while angular gyrus is also located at the parietal lobe. However, BNSS score was not significantly associated with whole-brain average Kw ($P = .4$).

Using BPRS to examine symptoms in SSD, whole-brain average Kw was not significantly associated with positive ($r = 0.20$, $P = .38$) or negative symptom scores ($r = -0.20$, $P = .37$). No significant regional effects were observed for positive symptoms (all $|r|<0.37$, $P > .05$), while negative symptoms subscale score was significant in the right superior corona radiata ($r = -0.49$, $P = .007$), consistent with BNSS findings.

Patients showed significantly reduced processing speed ($F = 19.5$, $P = 3\cdot\times 10^{-5}$) and working memory ($F = 10.9$, $P = 2 \times\cdot 10^{-3}$), which were not significantly associated with whole-brain average Kw (both $r \leq 0.21$, $P \geq .33$).

Endothelial Function

FMD was significantly reduced in SSD compared to HC (age and sex covaried in all analyses; $F_{3,64} = 19.6$, $P = 4 \times\cdot 10^{-5}$; **figure 3**), which remained significant after adding BMI[49] as a covariate ($P = .001$). Baseline ($P = .4$) and 1-minute post-occlusion ($P = .9$) arterial diameters were not statistically different between groups. FMD group differences remained significant after including baseline brachial diameter as a covariate ($P = 5 \times\cdot 10^{-5}$), suggested to be a potential confounding variable in FMD studies.[50] However, FMD was not significantly correlated with symptoms or cognitions (all $P > .05$).

Relationships Between Central Kw and Peripheral Endothelial Function

Whole-brain Kw in HC was not significantly associated with FMD ($r = 0.20$, $P = .4$), which does not support our original hypothesis and suggests that the central and peripheral vascular functions may be mediated through separate mechanisms. However, it is also possible that the underlying endothelial function may not impact all brain regions equally. Accordingly, we conducted additional regional explorations in a hypothesis generating framework. Positive correlations between Kw and FMD were found in ~94% of regions in HC, suggesting healthier peripheral endothelial function is associated with higher Kw under normal conditions (figures 4A and 4C). However, exploratory analyses showed that 3 regions were nominally significant ($P < .01$): left insula ($r = 0.55$, $P = .004$; figure 4B, top), right inferior frontal gyrus ($r = 0.55$, $P = .004$), and left external capsule ($r = 0.50$, $P = .009$). Meanwhile, over half (52%) of the regions in patients showed inverse associations with Kw, nominally significant at the left globus pallidus ($r = -0.48$, $P = .006$; figure 4B, middle). Whole-brain Kw in SSD was also not significantly associated with FMD ($r = 0.002$, $P = .99$). Further exploration

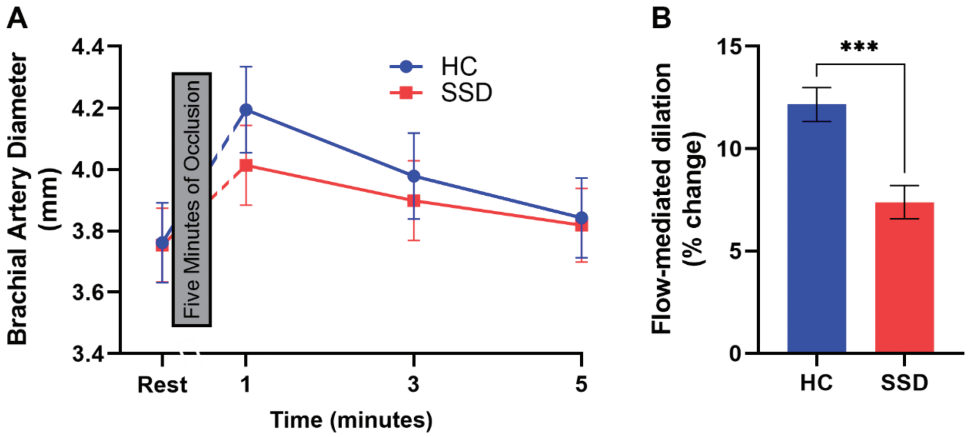

Fig. 3. Brachial artery flow-mediated dilation to assess endothelial function. (A) Brachial artery diameter was measured at rest and 1, 3, and 5 minutes after a 5-minute occlusion, adjusted for age, sex, and BMI. Break in x-axis represents the 5-minute occlusion. (B) The flow-mediated dilation (FMD) was significantly different between the two groups; *** $P < .001$. Error bars are SEM.

suggested that the number of regions showing positive versus negative associations was significantly different between SSD and HC ($\chi^2 = 46.5$, $P = <.0001$). The correlation coefficients were significantly different ($P < .01$) between groups in 6 regions (figure 4C; supplementary table 2), with the left putamen showing the greatest group differences (figure 4B, bottom).

Relationship with Other Demographic and Clinical Characteristics

Age was not associated with whole-brain average Kw in SSD or HC ($r = -0.08$, $P = .7$ and $r = -0.18$, $P = .4$, respectively), although older age was generally associated with lower Kw. Sex was not significantly associated with whole-brain average Kw in SSD or HC ($r = 0.19$, $P = .3$ and $r = 0.20$, $P = .3$, respectively). In group comparisons, whole-brain average Kw showed no significant age ($P = .40$) or age by diagnosis interaction ($P = .77$) effects. Similarly, with sex in group comparisons, whole-brain average Kw showed no significant sex main effect ($P = .18$) or diagnosis by sex interaction ($P = .76$).

Age was not associated with FMD in SSD or HC ($r = -0.17$, $P = .3$ and $r = -0.29$, $P = .1$, respectively), although older age was generally associated with lower FMD. Sex was not significantly associated with FMD in SSD or HC ($r = 0.02$, $P = .9$ and $r = 0.24$, $P = .19$, respectively). FMD showed a nominally significant age ($P = .05$), but no age by diagnosis interaction ($P = .54$) effects. Similarly, FMD showed no significant sex main effect ($P = .3$) or diagnosis by sex interaction ($P = .4$).

CPZ and whole-brain average Kw ($r = 0.14$, $P = .5$) or FMD ($r = 0.16$, $P = .4$) correlations were not significant. Smoking was not significantly associated with whole-brain average Kw ($r = 0.19$, $P = .37$) or FMD ($r = -0.19$, $P = .29$). Finally, cardiovascular measures (resting systolic and diastolic blood pressures and heart rate) were not significantly associated with whole-brain average Kw ($P = .4$–$.9$) or FMD ($P = .4$–$.8$). Further analyses to better understand these relationships are given in supplementary information. The significance level of patient-control differences in FMD ($P = .00001$ before, and $P = .00003$ after) and whole-brain Kw ($P = .007$ before, and $P = .04$ after) remained significant after adding age, gender, smoking, BMI, blood pressure, and heart rate as covariates in the respective regression models. Similarly, the correlations between negative symptoms and Kw of the right angular gyrus ($P = .006$ before, and $P = .006$ after) and superior corona radiata ($P = .001$ before, and $P = .001$ after) both remained significant with addition of these covariates as well.

Discussion

Whole-brain Kw and peripheral endothelial function were significantly reduced in patients with SSD compared to HC. The greatest deficits occurred right parietal areas. Reduced Kw in the right parietal angular gyrus and the underlying superior corona radiata white matter areas were significantly associated with negative symptoms. As expected, greater peripheral endothelial function was associated with higher brain Kw in nearly all regions in HC subjects, while the opposite relationship was found in over half of the brain regions in SSD, suggesting potentially altered neurovascular mechanisms in schizophrenia.

Brain network analysis previously demonstrated negative symptoms in treatment-naïve patients most strongly associated with right superior parietal lobe and frontoparietal dysconnectivity.[19] Moreover, right superior temporo-parietal junction cortical thinning is also associated with negative symptoms.[20] Together, right frontoparietal network hypo-activation/hypo-perfusion[16,19] have long been linked to negative symptoms, although without clear mechanistic understandings. Here, we found Kw deficits in SSD were most severe in specific right parietal locations, and negative symptom

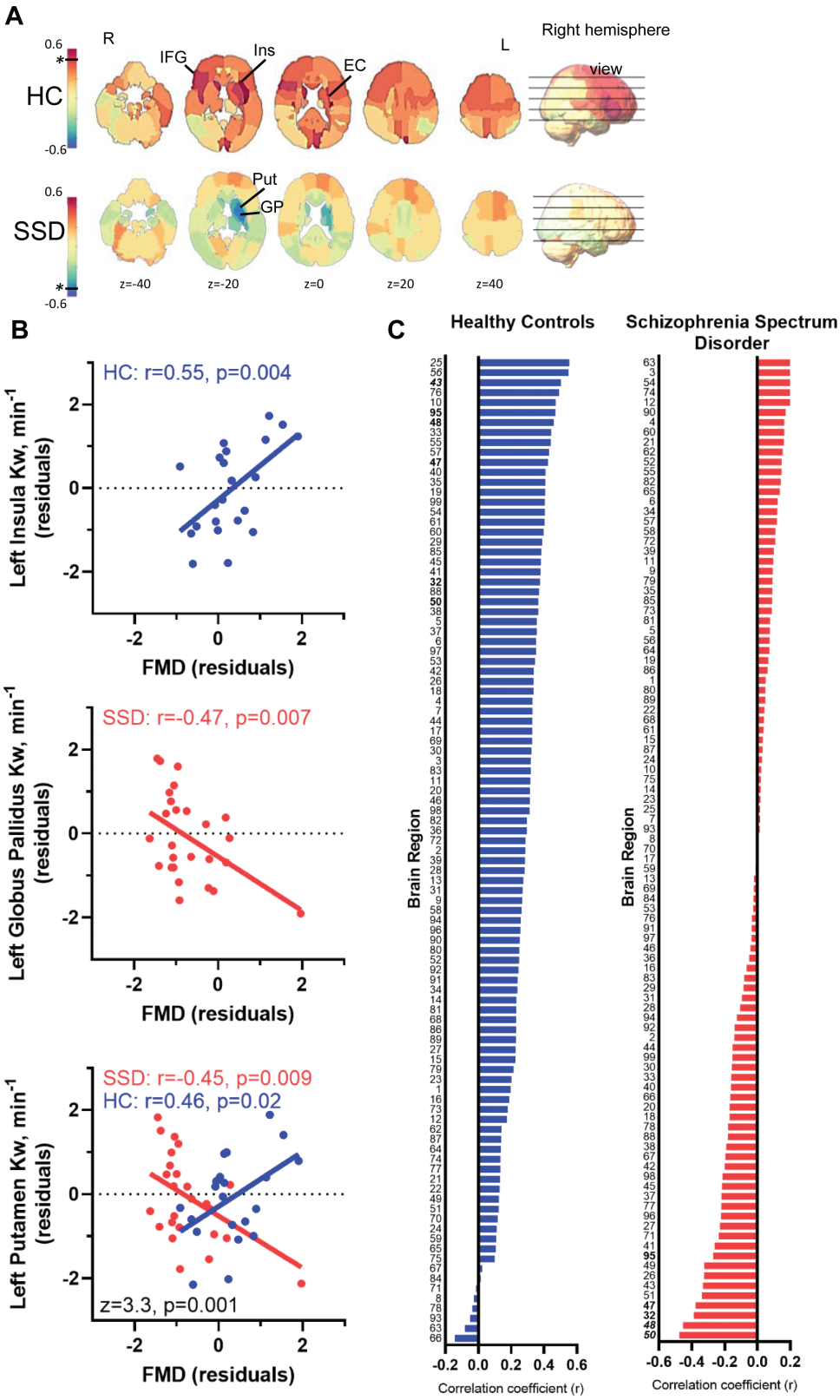

Fig. 4. Relationship between peripheral vascular endothelial function and cerebral water exchange measurements. (A) Mapping the whole-brain distributions of the relationship between flow-mediated dilation and water exchange (Kw) examined by linear regressions based on partial Pearson correlation *r*-values (covaried for age and sex). Colder colors indicate negative *r*-values; warmer colors indicate positive *r*-values. The black horizontal line and * represents the color corresponding to the $P < .01$, in either positive or negative direction, if present. (B) The most significant association found in controls, left insula (top), and patients, left globus pallidus (middle), and the greatest group difference in the correlation coefficients between FMD and Kw, left putamen (bottom), were plotted. (C) 99 brain regions' partial correlation coefficients (r), controlled for age and sex, arranged from greatest to least in HC (blue) and SSD (red) illustrating the overall pattern across brain regions. Names for each region are given in supplementary table 2. * significant *r*-value between FMD and Kw; # significant *z*-value for group differences in the correlation coefficients.

severity was most strongly associated with Kw reduction in the right parietal/angular gyrus and the right superior corona radiata, a tract connecting right frontoparietal areas. Right hemisphere Kw was numerically greater than the left in both HC and SSD, possibly reflecting an aspect of hemispheric dominance not previously explored in terms of BBB function, although hemispheric asymmetry is well-documented in many brain imaging findings in both normal and disease conditions.[51,52] These findings corroborate anatomic specificity for negative symptoms, offer new mechanistic hypotheses, and suggest that neurovascular water exchange abnormalities may be a crucial connection.

This is the first study reporting neurovascular water exchange dysfunction in SSD using DP-ASL. Clinical BBB imaging traditionally uses DCE-MRI, which detects large molecule BBB leakage unobserved in SSD.[4] In comparison, water has a smaller molecular weight. BBB trans-endothelial and perivascular water exchanges occur both passively and actively through specific water channels at the astrocytic processes.[53] It is thus hypothesized that imaging the water exchanges can provide more refined detection of BBB dysfunction[8,9] that is not limited to overt, large molecule leakage processes.

Animal and human studies have compared DP-ASL and DCE-MRI.[9,11] The primary measure by DCE-MRI is the volume transfer constant (K_{trans}) to estimate gadolinium leakage into the extravascular-extracellular space.[54,55] In post-ischemic stroke, K_{trans} was increased while Kw was reduced,[9] suggesting impeded water exchange mechanisms under models of substantial BBB disruption, further supported using high-dose mannitol treatment in rodents also showing reduced Kw.[56] The inverse association indicated that Kw was not measuring major BBB leakages of large molecules as in K_{trans},[11] but rather reduced water exchange functioning potentially due to impeded passages, disrupted neurovascular energy supplies, or other mechanisms. However, PET studies showed increased efflux of radiotracer molecule in the brain of patients with SSD, consistent with our findings.[57] Moreover, CSF biomarkers demonstrated increased BBB permeability in SSD compared to HC, based on cellular and protein-based assays.[58]

AQP-4 channels on astrocytic foot processes ensheath the cerebrovasculature as the primary active transporter of water in the brain.[53,59] These channels support glymphatic pathways for CSF flow along perivascular spaces, facilitating exchanges with brain parenchyma.[60] Overt BBB leakage indexed by increased K_{trans} may impede water flow registered by Kw. Therefore, both Kw and K_{trans} may measure BBB dysfunction but for different aspects. However, positive Kw and K_{trans} associations can be found in brain regions of preclinical small vessel diseases that have chronic BBB changes but without massive BBB disruption.[11] Therefore, the Kw and K_{trans} relationship appears dynamic and potentially depends on the BBB subcomponents being disrupted. Previous imaging studies have not addressed BBB subcomponent deficits in SSD, which is likely a missing opportunity because it is unlikely that SSD patients would have the same type of extensive BBB leakage as in major neurological insults.

DP-ASL studies have postulated that Kw may measure BBB endothelial integrity,[5–8,11,37] but with limited clinical evidence. Thus, we examined FMD, a validated peripheral endothelial function measure in cardiovascular conditions,[45,48] although its use to inform cerebrovascular mechanism is similarly unexplored. Here, higher Kw trended with higher FMD in HC in nearly all brain regions, supporting higher water exchange function related to better endothelial functions under normal conditions. In SSD, however, significantly more regions were negatively associated. The combination of reduced Kw, reduced FMD, and an inverse association between FMD and Kw in substantially more regions, compared to HC, provided initial evidence of an abnormal, potentially endothelia-mediated neurovascular water exchange mechanism in schizophrenia. Although no significant whole-brain Kw associations with FMD were observed, it is possible that specific brain regions may be more vulnerable to endothelia-mediated abnormalities, and caution is required when interpreting the exploratory findings at individual regions.

One speculation for the inverse relationship is that if patients had reduced AQP-4 functions, suggested by lower Kw, those patients with relatively higher levels of endothelial nitric oxide signaling (ie, higher FMD) would have pronounced capillary bed dilation. The combination would result in a relatively inflated Kw denominator (ie, volume of water tracer in capillary space). Consequently, reduced water transport in the parenchyma would be registered as a lower overall Kw, and an inverse Kw-FMD relationship would be produced. These findings were unexpected based on our initial hypothesis. However, an explanation for the seemingly counter-intuitive observation of inverse Kw and FMD relationships in SSD imply that a schizophrenia-specific endothelia process may occur in selected brain regions. Indeed, increased cerebral blood volume has been described in schizophrenia and is associated with clinical high-risk individuals later converting to psychosis, persisting after psychosis onset.[61] In parallel, AQP-4 channel abnormalities have also been implicated in SSD, with mutations possibly conferring dysfunctional properties,[62] and regional gene expression up-regulation as compensatory responses to excitotoxic molecule build-up.[63] Therefore, our results may implicate disturbed AQP-4 functions in SSD. AQP-4 may mediate part of the endothelial dysfunction registered in Kw, whereby unrelated mechanisms may be at play for endothelial dysfunction peripherally. Moreover, endothelial dysfunction may be shared in a range of peripheral disorders with otherwise distinct pathophysiology, like coronary artery disease,[64,65] psoriasis,[66,67] and obstructive sleep apnea.[68,69] Further basic neuroscience efforts are needed to better understand these findings.

Our study has several limitations. Antipsychotics may impact vascular measures better studied in medication-naive individuals. Sex, smoking, and cardiovascular factors have not been robustly associated with Kw in our data or specifically explored in previous Kw literature, representing needed further research. Endothelial measures are typically associated with metabolic/cardiovascular factors, and we may have only controlled for some potential confounds. Reduced FMD has been associated with smoking and obesity,[30,70–73] thus we may expect some Kw and FMD effects despite no statistical evidence found in our cohort, possibly due to sample size limitations. Although endothelial cells between peripheral and central vasculature share many similarities, distinctions exist[32,74,75] and the study did not directly measure endothelial functions at the BBB level. Kw likely registers many aspects of the neurovascular unit, not just the endothelial cell, and thus the use of FMD may only capture one feature of a complicated, and not fully discerned system. Handedness was not accounted for, and the cross-sectional design limits causal explanations. Lastly, the modest sample size of this pilot study, although adequately powered for the primary measure of whole-brain Kw, was underpowered to detect 99 brain regional analysis when fully corrected for multiple comparisons, and thus caution is required when interpreting regional specific findings in this more exploratory approach. Given the clinical importance, however, these findings encourage larger scaled, follow-up studies properly powered to investigate brain regions of interest, like the angular gyrus, that may contribute to symptomatic burdens commonly afflicting SSD populations.

In conclusion, this study demonstrated that combining central water exchange imaging with peripheral endothelial function assessments provide non-invasive, in vivo tools for informing previously undetected cerebrovascular abnormalities in SSD. In conjunction with an association with negative symptoms, our findings suggest neurovascular dysfunction may be a key target for novel therapeutic development. Finally, as endothelial dysfunctions are predictive of subsequent cardiovascular diseases, the endothelial and neurovascular BBB dysfunction hypothesis examined here may also be relevant to the increased risks for cardio-metabolic diseases that SSD patients disproportionally suffer.[76]

Supplementary Material

Supplementary material is available at https://academic.oup.com/schizophreniabulletin/.

Funding

Sources of funding and support include University of Maryland/ Sheppard Pratt Psychiatry Residency PSTP Program (E.G.); NIMH R01MH116948 (L.E.H.); NINDS RF1NS114628 (L.E.H., P.K., and B.M.); NIMH R01MH112180 (L.E.H.); NINDS R01NS114382 (D.J.J.W.); NINDS R01 RF1NS122028 (D.J.J.W.).

Acknowledgments

L.E.H. has received or is planning to receive research funding or consulting fees from Mitsubishi, Your Energy Systems LLC, Neuralstem, Taisho, Heptares, Pfizer, Luye Pharma, Sound Pharma, IGC Pharma, Takeda, and Regeneron. A.R.S. is an employee of Regeneron Pharmaceuticals, Inc. and receives salary, stock and stock options as compensation. All other authors declare no financial interests that could represent a conflict of interest.

References

1. Greene C, Kealy J, Humphries MM, *et al*. Dose-dependent expression of claudin-5 is a modifying factor in schizophrenia. *Mol Psychiatry.* 2018;23(11):2156–2166.
2. Uranova NA, Vikhreva OV, Rachmanova VI, Orlovskaya DD. Ultrastructural alterations of myelinated fibers and oligodendrocytes in the prefrontal cortex in schizophrenia: a postmortem morphometric study. *Schizophr Res Treatment.* 2011;2011:325789.
3. Pong S, Karmacharya R, Sofman M, Bishop JR, Lizano P. The role of brain microvascular endothelial cell and blood-brain barrier dysfunction in schizophrenia. *Complex Psychiatry.* 2020;6(1-2):30–46.
4. Szymanski S, Ashtari M, Zito J, Degreef G, Bogerts B, Lieberman J. Gadolinium-DTPA enhanced gradient echo magnetic resonance scans in first episode of psychosis and chronic schizophrenic patients. *Psychiatry Res. Neuroimaging.* 1991;40(3):203–207.
5. Shao X, Ma SJ, Casey M, D'Orazio L, Ringman JM, Wang DJJ. Mapping water exchange across the blood-brain barrier using 3D diffusion-prepared arterial spin labeled perfusion MRI. *Magn Reson Med.* 2019;81(5):3065–3079.
6. Palomares JA, Tummala S, Wang DJ, *et al*. Water exchange across the blood-brain barrier in obstructive sleep apnea: an MRI diffusion-weighted pseudo-continuous arterial spin labeling study. *J Neuroimaging.* 2015;25(6):900–905.
7. Gold BT, Shao X, Sudduth TL, *et al*. Water exchange rate across the blood-brain barrier is associated with CSF amyloid-β 42 in healthy older adults. *Alzheimers Dement.* 2021;17:2020–2029.
8. Ford JN, Zhang Q, Sweeney EM, *et al*. Quantitative water permeability mapping of blood-brain-barrier dysfunction in aging. *Front Aging Neurosci.* 2022;14:867452.
9. Tiwari YV, Lu J, Shen Q, Cerqueira B, Duong TQ. Magnetic resonance imaging of blood-brain barrier permeability in ischemic stroke using diffusion-weighted arterial spin labeling in rats. *J Cereb Blood Flow Metab.* 2017;37(8):2706–2715.
10. Tiwari YV, Shen Q, Jiang Z, *et al*. Measuring blood-brain-barrier permeability using Diffusion-Weighted Arterial Spin Labeling (DW-ASL): corroboration with Ktrans and Evan's blue measurements. *Proc Intl Soc Magn Reson Med.* 2015;23:0792–0792.

11. Shao X, Jann K, Ma SJ, *et al*. Comparison between blood-brain barrier water exchange rate and permeability to gadolinium-based contrast agent in an elderly cohort. *Front Neurosci.* 2020;14:1–16.
12. Uchida Y, Kan H, Sakurai K, *et al*. APOE ε4 dose associates with increased brain iron and β-amyloid via blood-brain barrier dysfunction. *J Neurol Neurosurg Psychiatry.* 2022.
13. Li Y, Ying Y, Yao T, *et al*. Decreased water exchange rate across blood-brain barrier in hereditary cerebral small vessel disease. *Brain.* 2023.
14. Sabri O, Erkwoh R, Schreckenberger M, *et al*. Regional cerebral blood flow and negative/positive symptoms in 24 drug-naive schizophrenics. *J Nucl Med.* 1997;38(2):181–188.
15. Pinkham A, Loughead J, Ruparel K, *et al*. Resting quantitative cerebral blood flow in schizophrenia measured by pulsed arterial spin labeling perfusion MRI. *Psychiatry Res.* 2011;194(1):64–72.
16. Andreasen NC, Rezai K, Alliger R, *et al*. Hypofrontality in neuroleptic-naive patients and in patients with chronic schizophrenia. Assessment with xenon 133 single-photon emission computed tomography and the Tower of London. *Arch Gen Psychiatry.* 1992;49(12):943–958.
17. Lahti AC, Holcomb HH, Medoff DR, Weiler MA, Tamminga CA, Carpenter WT, Jr. Abnormal patterns of regional cerebral blood flow in schizophrenia with primary negative symptoms during an effortful auditory recognition task. *Am J Psychiatry.* 2001;158(11):1797–1808.
18. Sklar AL, Coffman BA, Salisbury DF. Fronto-parietal network function during cued visual search in the first-episode schizophrenia spectrum. *J Psychiatr Res.* 2021;141:339–345.
19. Zhou M, Zhuo L, Ji R, *et al*. Alterations in functional network centrality in first-episode drug-naïve adolescent-onset schizophrenia. *Brain Imaging Behav.* 2022;16(1):316–323.
20. Bodnar M, Hovington CL, Buchy L, Malla AK, Joober R, Lepage M. Cortical thinning in temporo-parietal junction (TPJ) in non-affective first-episode of psychosis patients with persistent negative symptoms. *PLoS One.* 2014;9(6):e101372.
21. Li X, Tang J, Wu Z, Zhao G, Liu C, George MS. SPECT study of Chinese schizophrenic patients suggests that cerebral hypoperfusion and laterality exist in different ethnic groups. *World J Biol Psychiatry.* 2005;6(2):98–106.
22. Greyling A, van Mil ACCM, Zock PL, Green DJ, Ghiadoni L, Thijssen DH; TIFN International Working Group on Flow Mediated Dilation. Adherence to guidelines strongly improves reproducibility of brachial artery flow-mediated dilation. *Atherosclerosis.* 2016;248:196–202.
23. Thijssen DH, Black MA, Pyke KE, *et al*. Assessment of flow-mediated dilation in humans: a methodological and physiological guideline. *Am J Physiol Heart Circ Physiol.* 2011;300(1):H2–12.
24. Inaba Y, Chen JA, Bergmann SR. Prediction of future cardiovascular outcomes by flow-mediated vasodilatation of brachial artery: a meta-analysis. *Int J Cardiovasc Imaging.* 2010;26(6):631–640.
25. Reif A, Herterich S, Strobel A, *et al*. A neuronal nitric oxide synthase (NOS-I) haplotype associated with schizophrenia modifies prefrontal cortex function. *Mol Psychiatry.* 2006;11(3):286–300.
26. Nakano Y, Yoshimura R, Nakano H, *et al*. Association between plasma nitric oxide metabolites levels and negative symptoms of schizophrenia: a pilot study. *Hum Psychopharmacol.* 2010;25(2):139–144.
27. Alley H, Owens CD, Gasper WJ, Grenon SM. Ultrasound assessment of endothelial-dependent flow-mediated vasodilation of the brachial artery in clinical research. *J Vis Exp.* 2014;52070(92):e52070.
28. Faulx MD, Wright AT, Hoit BD. Detection of endothelial dysfunction with brachial artery ultrasound scanning. *Am Heart J.* 2003;145(6):943–951.
29. Uehata A, Lieberman EH, Gerhard MD, *et al*. Noninvasive assessment of endothelium-dependent flow-mediated dilation of the brachial artery. *Vasc Med.* 1997;2(2):87–92.
30. Celermajer DS, Sorensen KE, Gooch VM, *et al*. Non-invasive detection of endothelial dysfunction in children and adults at risk of atherosclerosis. *Lancet.* 1992;340(8828):1111–1115.
31. Zeiher AM, Drexler H, Saurbier B, Just H. Endothelium-mediated coronary blood flow modulation in humans. Effects of age, atherosclerosis, hypercholesterolemia, and hypertension. *J Clin Invest.* 1993;92(2):652–662.
32. Paik DT, Tian L, Williams IM, *et al*. Single-cell RNA sequencing unveils unique transcriptomic signatures of organ-specific endothelial cells. *Circulation.* 2020;142(19):1848–1862.
33. Kirkpatrick B, Strauss GP, Nguyen L, *et al*. The brief negative symptom scale: psychometric properties. *Schizophr Bull.* 2011;37(2):300–305.
34. Overall JE, Gorham DR. The brief psychiatric rating scale. *Psychol Rep.* 1962;10(3):799–812.
35. Wechsler D. *Wechsler Adult Intelligence Scale-Third Edition and Wechsler Memory Scale—Third Edition Technical Manual*. San Antonio: Pearson, TX; 1997b.
36. Knowles EE, David AS, Reichenberg A. Processing speed deficits in schizophrenia: reexamining the evidence. *Am J Psychiatry.* 2010;167(7):828–835.
37. St Lawrence KS, Owen D, Wang DJ. A two-stage approach for measuring vascular water exchange and arterial transit time by diffusion-weighted perfusion MRI. *Magn Reson Med.* 2012;67(5):1275–1284.
38. Wang J, Alsop DC, Song HK, *et al*. Arterial transit time imaging with flow encoding arterial spin tagging (FEAST). *Magn Reson Med.* 2003;50(3):599–607.
39. Spann SM, Shao X, Wang DJJ, *et al*. Robust single-shot acquisition of high resolution whole brain ASL images by combining time-dependent 2D CAPIRINHA sampling with spatio-temporal TGV reconstruction. *NeuroImage*. 2020;206:116337.
40. Lu H, Clingman C, Golay X, van Zijl PCM. Determining the longitudinal relaxation time (T1) of blood at 3.0 Tesla. *Magn Reson Med.* 2004;52(3):679–682.
41. Lim IAL, Faria AV, Li X, *et al*. Human brain atlas for automated region of interest selection in quantitative susceptibility mapping: application to determine iron content in deep gray matter structures. *Neuroimage.* 2013;82:449–469.
42. Vaden KI, Jr, Gebregziabher M, Kuchinsky SE, Eckert MA. Multiple imputation of missing fMRI data in whole brain analysis. *Neuroimage.* 2012;60(3):1843–1855.
43. van Buuren S, Groothuis-Oudshoorn K. mice: multivariate imputation by chained equations in R. *J Stat Softw.* 2011;45(3):1– 67.
44. Hyun JW, Li Y, Gilmore JH, Lu Z, Styner M, Zhu H. SGPP: spatial Gaussian predictive process models for neuroimaging data. *Neuroimage.* 2014;89:70–80.
45. Corretti MC, Anderson TJ, Benjamin EJ, *et al*; International Brachial Artery Reactivity Task Force. Guidelines for the ultrasound assessment of endothelial-dependent flow-mediated vasodilation of the brachial artery: a report of the International Brachial Artery Reactivity Task Force. *J Am Coll Cardiol.* 2002;39(2):257–265.

46. Lima BB, Quyyumi AA, Vaccarino V. A future for flow-mediated dilation—just follow the guidelines—reply. *JAMA Cardiol.* 2020;5(3):361–361.
47. Vetter MW, Martin B-J, Fung M, Pajevic M, Anderson TJ, Raedler TJ. Microvascular dysfunction in schizophrenia: a case-control study. *NPJ Schizophr.* 2015;1:15023–15023.
48. Salimi S, Yanosky JD, Huang D, *et al*. Long-term exposure to particulate air pollution and brachial artery flow-mediated dilation in the Old Order Amish. *Environ Health.* 2020;19(1):50.
49. Williams IL, Chowienczyk PJ, Wheatcroft SB, *et al*. Endothelial function and weight loss in obese humans. *Obes Surg.* 2005;15(7):1055–1060.
50. Atkinson G, Batterham AM, Thijssen DH, Green DJ. A new approach to improve the specificity of flow-mediated dilation for indicating endothelial function in cardiovascular research. *J Hypertens.* 2013;31(2):287–291.
51. Angrilli A, Spironelli C, Elbert T, Crow TJ, Marano G, Stegagno L. Schizophrenia as failure of left hemispheric dominance for the phonological component of language. *PLoS One.* 2009;4(2):e4507.
52. Tiihonen J, Katila H, Pekkonen E, *et al*. Reversal of cerebral asymmetry in schizophrenia measured with magnetoencephalography. *Schizophr Res.* 1998;30(3):209–219.
53. Papadopoulos MC, Verkman AS. Aquaporin water channels in the nervous system. *Nat Rev Neurosci.* 2013;14(4):265–277.
54. Dewey BE, Xu X, Knutsson L, *et al*. MTT and blood-brain barrier disruption within asymptomatic vascular WM lesions. *Am J Neuroradiol.* 2021;42(8):1396–1402.
55. Li W, Long JA, Watts LT, *et al*. A quantitative MRI method for imaging blood-brain barrier leakage in experimental traumatic brain injury. *PLoS One.* 2014;9(12):e114173e114173.
56. Burks SR, Kersch CN, Witko JA, *et al*. Blood–brain barrier opening by intracarotid artery hyperosmolar mannitol induces sterile inflammatory and innate immune responses. *Proc Natl Acad Sci USA.* 2021;118(18):e2021915118.
57. de Klerk OL, Willemsen ATM, Bosker FJ, *et al*. Regional increase in P-glycoprotein function in the blood-brain barrier of patients with chronic schizophrenia:: a PET study with [11C]verapamil as a probe for P-glycoprotein function. *Psychiatry Res Neuroimaging.* 2010;183(2):151–156.
58. Jeppesen R, Orlovska-Waast S, Sørensen NV, Christensen RHB, Benros ME. Cerebrospinal fluid and blood biomarkers of neuroinflammation and blood-brain barrier in psychotic disorders and individually matched healthy controls. *Schizophr Bull.* 2022;48(6):1206–1216.
59. Szentistványi I, Patlak CS, Ellis RA, Cserr HF. Drainage of interstitial fluid from different regions of rat brain. *Am J Physiol.* 1984;246(6 Pt 2):F835–844.
60. Iliff JJ, Wang M, Liao Y, *et al*. A paravascular pathway facilitates CSF flow through the brain parenchyma and the clearance of interstitial solutes, including amyloid β. *Sci Transl Med.* 2012;4(147):147ra–14111.
61. Talati P, Rane S, Skinner J, Gore J, Heckers S. Increased hippocampal blood volume and normal blood flow in schizophrenia. *Psychiatry Res Neuroimaging.* 2015;232(3):219–225.
62. Wu YF, Sytwu HK, Lung FW. Human Aquaporin 4 gene polymorphisms and haplotypes are associated with serum S100B level and negative symptoms of schizophrenia in a southern Chinese Han population. *Front Psychiatry.* 2018;9:657.
63. Ericek OB, Akillioglu K, Saker D, *et al*. Distribution of Aquaporin-4 channels in hippocampus and prefrontal cortex in mk-801-treated balb/c mice. *Ultrastruct Pathol.* 2022;46(1):63–79.
64. Manganaro A, Ciracì L, Andrè L, *et al*. Endothelial dysfunction in patients with coronary artery disease: insights from a flow-mediated dilation study. *Clin Appl Thromb Hemost.* 2014;20(6):583–588.
65. Heiss C, Rodriguez-Mateos A, Bapir M, Skene SS, Sies H, Kelm M. Flow-mediated dilation reference values for evaluation of endothelial function and cardiovascular health. *Cardiovasc Res.* 2023;119(1):283–293.
66. Garshick MS, Tawil M, Barrett TJ, *et al*. Activated platelets induce endothelial cell inflammatory response in psoriasis via COX-1. *Arterioscler Thromb Vasc Biol.* 2020;40(5):1340–1351.
67. De Simone C, Di Giorgio A, Sisto T, *et al*. Endothelial dysfunction in psoriasis patients: cross-sectional case-control study. *Eur J Dermatol.* 2011;21(4):510–514.
68. Jelic S, Lederer DJ, Adams T, *et al*. Vascular inflammation in obesity and sleep apnea. *Circulation.* 2010;121(8):1014–1021.
69. Wang Y, Xu H, Qian Y, Guan J, Yi H, Yin S. Patients with obstructive sleep apnea display decreased flow-mediated dilatation: evidence from a meta-analysis. *Med Sci Monit.* 2017;23:1069–1082.
70. Cui M, Cui R, Liu K, *et al*; CIRCS investigators. Associations of tobacco smoking with impaired endothelial function: the Circulatory Risk in Communities Study (CIRCS). *J Atheroscler Thromb.* 2018;25(9):836–845.
71. Ijzerman RG, Serne EH, van Weissenbruch MM, de Jongh RT, Stehouwer CD. Cigarette smoking is associated with an acute impairment of microvascular function in humans. *Clin Sci.* 2003;104(3):247–252.
72. Selim M, Jones R, Novak P, Zhao P, Novak V. The effects of body mass index on cerebral blood flow velocity. *Clin Auton Res.* 2008;18(6):331–338.
73. Singh SS, Roeters-van Lennep JE, Lemmers RFH, *et al*. Sex difference in the incidence of microvascular complications in patients with type 2 diabetes mellitus: a prospective cohort study. *Acta Diabetol.* 2020;57(6):725–732.
74. Hou S, Li Z, Dong J, *et al*. Heterogeneity in endothelial cells and widespread venous arterialization during early vascular development in mammals. *Cell Res.* 2022.
75. Vanlandewijck M, He L, Mäe MA, *et al*. A molecular atlas of cell types and zonation in the brain vasculature. *Nature.* 2018;554(7693):475–480.
76. Correll CU, Solmi M, Veronese N, *et al*. Prevalence, incidence and mortality from cardiovascular disease in patients with pooled and specific severe mental illness: a large-scale meta-analysis of 3,211,768 patients and 113,383,368 controls. *World Psychiatry.* 2017;16(2):163–180.